

Examine the Properties of Nanostructured Ni, Mn, and Co Synthesized Materials using precipitation method and synthesized material used battery.

Mr. Serfraz Najeer Shaikh

Electronics and Communication Engg.
Dr.APJ Abdul Kalam University, Indore, India
Indore, India
e-mail: serfrazshaikh@gmail.com

Dr. Rahul Mishra

Electronics and Communication Engg.
Dr.APJ Abdul Kalam University, Indore, India
Indore, India
e-mail: rahulmishra@aku.ac.in

Abstract- Libatteries are secondary batteries containing a lithium anode and Li^+ ions dissolved in carbon. The cathode material contains a solution that releases lithium. With high energy density and low resistivity, it is "one of the three types of electric power acid, or battery, and is heavy and has more energy than nickel-ion batteries." Twice the size of a hydrogen battery, it is only half the size and weight of a nickel-metal hydride battery for the same energy. These advantages make lithium ion batteries an important factor in driving the technological revolution. Lithium-ion batteries also work well in temperatures from 20 degrees Celsius to +50 degrees Celsius and can withstand hundreds of charges and discharges. In this paper we are using nano material $(\text{Ni}_{0.25}\text{Mn}_{0.75})\text{CO}_3$ for synthesis to get the porous nano material, that synthesized nano porous material we are characterizing under different technique to know the characteristics of that material like size and shape, thermal effect and other. The same material will be used to prepare battery and the performance of that battery will be analysed and study on the performance will be done.

Keywords- Batteries, synthesis, porous material, nano cube, thermogravimetric analysis.

1. POROUS LNMO NANOCUBES PRODUCTION

The spongy LNMO nanocubes were made from the precursor $(\text{Ni}_{0.25}\text{Mn}_{0.75})\text{CO}_3$ nanocubes. The $(\text{Ni}_{0.25}\text{Mn}_{0.75})\text{CO}_3$ nanocubes precursor was made using a simple carbonate and sulphate precipitation process, in which an aqueous solution of Nickel sulphate ($\text{NiSO}_4\cdot\text{H}_2\text{O}$, Merck, 98.50 percent) and Manganese sulphate ($\text{MnSO}_4\cdot\text{H}_2\text{O}$, Merck > 98.50 percent) ($\text{Ni}^{2+}/\text{Mn}^{2+}$ Cationic ratio 1 as to 3) (Cationic ratio Solution B-), including 0.30 mM aqueous sodium carbonate (Na_2CO_3 -Merck, 98.5 percent and sodium sulphate (Na_2SO_4 , Merck, 98.5 percent), was made in the meantime by stirring for 1 hour at room temperature. Under steady stirring for 3 hours, the solution B- was added drip wise to the solution A holding Ni^{2+} & Mn^{2+} cations to generate $(\text{Ni}_{0.25}\text{Mn}_{0.75})\text{CO}_3$ nanocubes originator, resulting in a soft nimble green colour precipitous. The generated product was centrifuged, rinsed multiple times with water and ethanol, then dried for 24 hours in a void furnace at 101 °C. For the creation of porous $\text{LiNi}_{0.5}\text{Mn}_{1.5}\text{O}_4$ microcubes, a stoichiometric amount of LiOH was combined

through the obtained $(\text{Ni}_{0.25}\text{Mn}_{0.75})\text{CO}_3$ naocubes predecessor and calcined at 810 °C for 11 hours. Figure 1 shows a schematic diagram for the synthesis of porous $\text{LiNi}_{0.5}\text{Mn}_{1.5}\text{O}_4$ nanocubes. For structural and electrochemical characterizations, the produced porous LNMO microcubes were maintained in a vacuum desiccator.

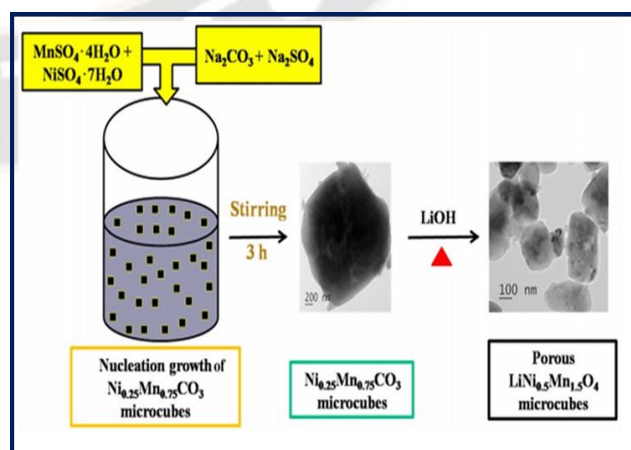


Figure. 1. Schematic diagram over precipitation method of microcubes

2. RESULT AND DISCUSSION

2.1 THERMOGRAVIMETRIC ANALYSIS

The produced $(\text{Ni}_{0.25}\text{Mn}_{0.75})\text{CO}_3 + \text{LiOH}$ combination underwent thermo gravimetric analysis (TGA), and the resultant spectrum is depicted in Figure 2.1 Weight loss occurs in three stages, each with a different temperature : 28-210 degrees Celsius, 210-351. degrees Celsius, and 351-651 degrees Celsius. The hygroscopicity and chemically bound water of LNMO microcubes causes an initial loss of 24% between 27 and 212 °C, resultant in water contain loss.

At 210-350 °C, the carbonate ($-\text{CO}_3$ group) employed in synthesis is completely removed, explaining the subsequent weight loss of roughly 25%. At 350-652 °C, a third weight-loss zone may exist because Mn_3O_4 is being broken down into MnO_2 .

No sluggishness was observed at 652-1000 degrees Celsius, indicating that the LNMO structure is stable at higher temperatures; therefore, the calcination temperature was adjusted during the synthesis of spinel porous LNMO microcube at 800 degrees Celsius.

Table no-1 Thermo gravimetric analysis based on temperature.

| Sr.no | Weight | Temperature of oven | Weight after heating in oven | % weight drop | REASON |
|-------|--------|---------------------|------------------------------|---------------|--------------------------------|
| 1 | 10g | 28 – 210 C | 7.6g | 24% | Chemical water loss |
| 2 | 7.6g | 210-350 C | 5.1g | 25% | Removal of carbonate |
| 3 | 5.1g | 350-650 C | 2g | 31% | Decomposition of Mn_4 |
| 4 | 2g | 650-1000 C | 2g | NO LOSS | |

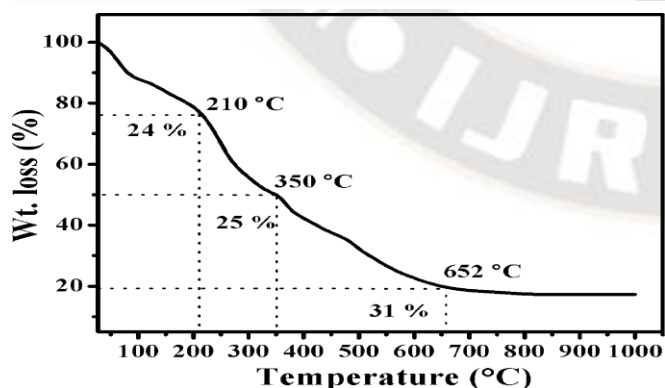


Figure 2.1 TGA arc of predecessor blend sample

2.2 X-RAY DIFFRACTION EXAMINATION

Figure 2.2 a,b shows the residue X-ray diffraction patterns of the composite $(\text{Ni}_{0.25}\text{Mn}_{0.75})\text{CO}_3$ and the obtained

LNMO nanocubes, respectively. $(\text{Ni}_{0.25}\text{Mn}_{0.75})$ the diffraction peaks in CO_3 canister be indexed to the hexagonal structure with the R-3c cosmos set (Figure 2.2a), $\text{LiNi}_{0.5}\text{Mn}_{1.5}\text{O}_4$ indexed to a spinel arrangement with a cosmos group of fd-3m (Figure 2.2 b). Diffraction peaks with greater sharpness and intensity revealed that the porous LNMO microcubes were extremely crystalline. The secondary phase of $\text{Li}_x\text{Ni}_{1-x}\text{O}$ or NiO , whose products are often seen to rise with increasing the Mn/Ni ratio, may be responsible for the development of asterisk peaks at 37.6° . At the same time, Li ions were lost from the spongy LNMO microcubes during great hotness calcinations because of the decrease in Mn ion concentration. The Scherer equation yields an middling crystallite size of 54.9 nm for the synthetic porous LNMO microcubes.

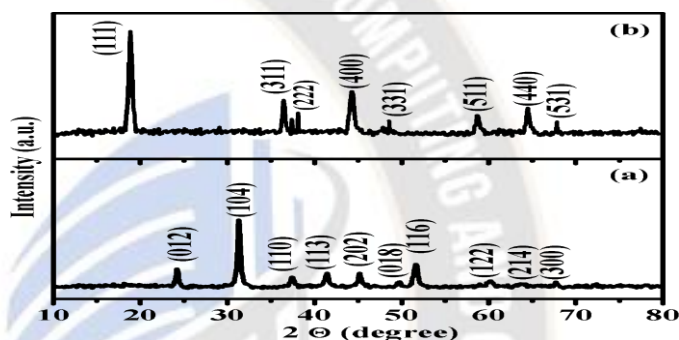


Figure 2.2 XRD shape of synthesized predecessor nanocubes (a) and created spongy LNMO nanocubes (b)

2.3 FE-SEM AND TEM ANALYSIS

Field emission scanning electron microscopy (FE-SEM) and transmission electron microscopy (TEM) were used to examine the morphology of the produced spongy $\text{LiNi}_{0.5}\text{Mn}_{1.5}\text{O}_4$ microcubes. FE-SEM images of LNMO (Figure 2.3 a, b) taken at low and high magnifications, respectively, show that the $\text{LiNi}_{0.5}\text{Mn}_{1.5}\text{O}_4$ invention is made up of uniformly scattered microcubes middling size of 163. nm.

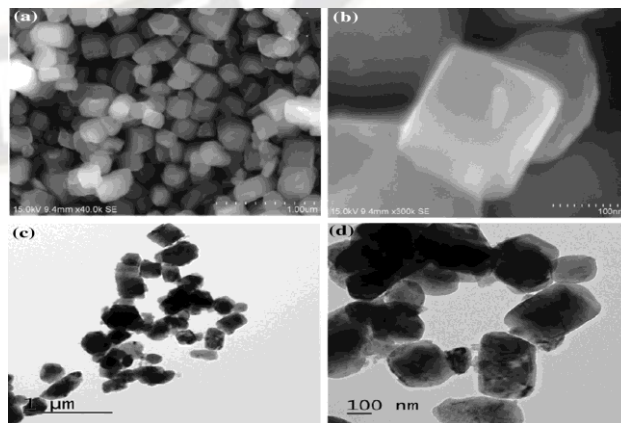


Figure 2.3 FESEM pictures of spongy LNMO nanocubes at diverse enlargements (a&b) and TEM pictures of spongy LNMO nanocubes at diverse enlargements (c&d)

The TEM pictures of porous LiNi_{0.5}Mn_{1.5}O₄ micro-cubes produced are shown in Figure 2.3 c, d, and they confirm the FE-SEM pictures showing that the shape of the produced LNMO is that of spongy micro-cubes. Ni_{0.25}Mn_{0.75}CO₃ particles have a cubic shape as synthesized.

2.4 BET ANALYSIS

The precise apparent area of the porous LNMO microcubes was determined by performing a Brunauer –Emmett -Teller measurement utilizing N₂ adsorption/desorption isotherm analysis (Figure 2.4 a).

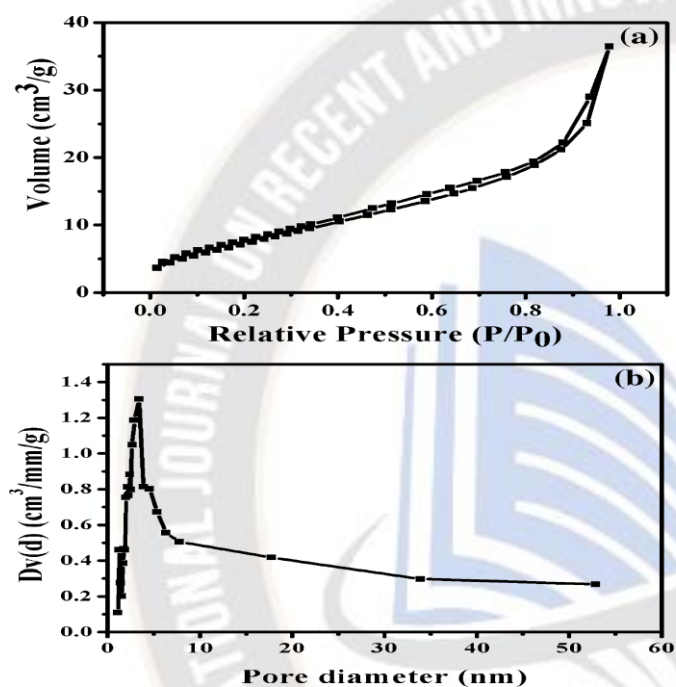


Figure 2.4 NAD forward-facing of spongy LNMO nanocubes (a) and B.J.H dispersal arcs of LNMO nanocubes rendering nitrogen front (b)

A nano-porous dimension of 1.3801 nm and a pore capacity 3.6201 cm³ g⁻¹ are shown for the LNMO micro-cubes in Figure 2.4b. Additionally, the microcubes are organized with uniform positioning between surrounding spongy microcubes, which facilitates

Efficient electron and ion movement and, in turn, better electrochemical performance in batteries and supercapacitors.

2.5 ELECTROCHEMICAL PERFORMANCE IN LI-ION BATTERY

Assembling CR2032 coin cells allowed us to examine the LNMO cathodes in partial chamber lithium-ion cells using recurring voltammetry and charging-discharging measurement, providing insight into the microcubes' electrochemical performance after synthesis.

The CV curve of LNMO microcubes at a test rate of 0.10 mV s⁻¹ is shown in Figure 2.5 over a probable range of 3.50-5.0 V. Smaller peaks arise between 3.80 and 4.05 V, which is

consistent with the presence of Mn⁴⁺/Mn³⁺, whereas the larger peaks appear in the high voltage range.

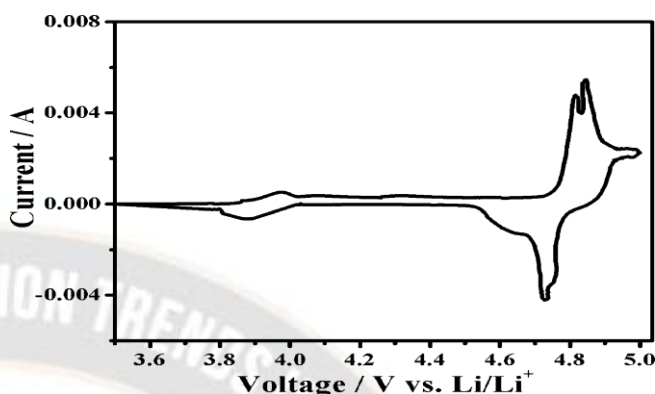


Figure 2.5 Cyclic voltammogram of the porous LNMO microcubes in the voltage range of 3.5–5.0 V at a scan rate of 0.1 mV s⁻¹

Ni²⁺/Ni³⁺ and Ni³⁺/Ni⁴⁺ redox pair contribute the most to the over-all volume and the entire drive, respectively, of the peaks at 4.70 V, explaining why the integrated area of the peaks at 4 V is substantially lower. According to our study, the LNMO nanocubes elements are the fd-3.0m planetary collection, and the Ni and Mn ions were randomly dispersed in the quartz structure, as illustrated above. The XRD measurements that validated the fd-3m structure of LNMO crystals show a strong correlation with the observed disorder behavior.

Figure 2.5 a displays charge-discharge curves obtained at 1 C rate in room temperature amongst 3.50V and 5.0V versus Li⁺/Li at 1.0C frequency for the great operating power of spongy LNMO microcubes cathode electrodes. Currently purified LNMO displays an very high working power of 5.0V, which means a upper drive density can be detailed when LNMO ingredients are used as cathode material in Li_{ion} battery.

Table no-2 current density based on number of cycle.

| No of cycle | Discharge Current | Capacity retention |
|-------------|-------------------|--------------------|
| 1 | 138.4 mA | 100% |
| 10 | 134.1 mA | 96.89% |
| 20 | 128.5 mA | 92.84 % |
| 25 | 122.5 mA | 88.51% |
| 35 | 115.3 mA | 83.30% |
| 45 | 108.1 mA | 78.10% |
| 50 | 103.2 mA | 74.56 % |

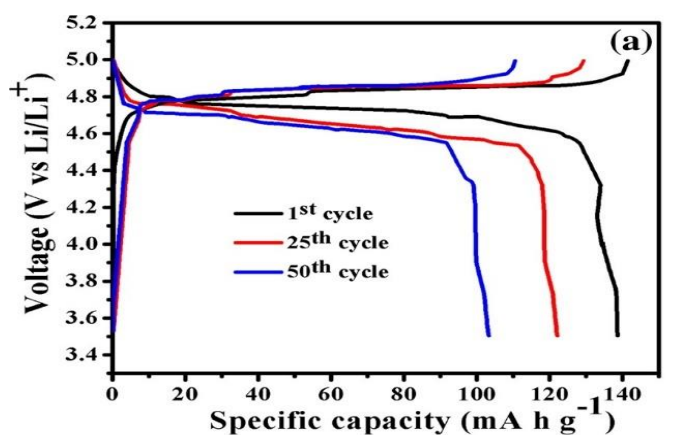


Figure 2.6 Charging-discharging arcs of spongy LNMO nanocubes at 1.0C in the impending sort of Voltage (a)

This is in contrast to more conventional cathode ingredients, such as Li_2CoO_2 (3.8 V), $\text{Li}_2\text{Mn}_2\text{O}_4$ (4.2 V), and Li_2FePO_4 (3.50 V). At 1.C rate, the charge-discharge profile of LNMO microcubes reveals a very extraordinary release capability of 138.40, 122.50, and 103.20 mA h g^{-1} , correspondingly, after 1, 10, 25, various cycles.

In Figure 2.7 b, we can see that the synthesized LNMO microcubes are both cyclically stable and coulombically efficient. We have performed over 50 constant series at 1 C speed to examine the cyclic stability; after these cycles, the LNMO nanocubes' specific capacity is 103.01 mA h g^{-1} and the competency holding is 73.9 close to 74.0 percentage. In addition, the breakdown of electrolytes at the higher potential reduces the coulombic efficiency of the produced cathode material from 97.3% after the first cycle to 93.12% after 51 cycles. These retentions, while still low, are greater than those reported in previous studies of LNMO-based cathode materials. High capacity retention and improved cycle stability may result from the porous structure of LNMO microcubes, which provides a robust underlay for the recurrent Li intercalation/de-intercalation processes.

Table no-3 charge and discharge current.

| No of cycle | Discharge Current (mA) | Charging Current (mA) | Columbic efficiency (%) |
|-------------|------------------------|-----------------------|-------------------------|
| 1 | 138.4 | 142.2 | 97.32 |
| 10 | 134.1 | 137.9 | 97.24 |
| 20 | 128.5 | 131.8 | 97.49 |
| 25 | 122.5 | 126.4 | 96.91 |
| 35 | 115.3 | 120.1 | 96.03 |
| 45 | 108.1 | 114.2 | 94.65 |
| 50 | 103.2 | 110.6 | 93.12 |

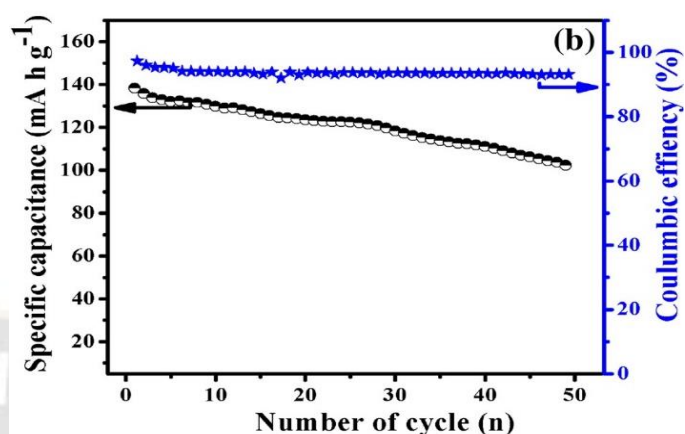


Figure 2.7 (b) coulombic proficiency related to spongy LNMO nanocubes

To further investigate the electrochemical kinetics of the LNMO microcubes, we conducted electrochemical impedance spectroscopy (EIS) tests in the frequency series of 10.0Hz to 101 KHz (Figure 2.8 Electrochemical impedance spectroscopy of many spongy LNMO nanocubes). Figure 2.8 depicts the Nyquist plot for the impedance spectra of the LNMO cathode resources attained at first cycle & fiftyth cycles.

Using the results of the EIS test, ZAVIEW software was able to construct an analogous circuit and calculate the precise resistance from each source. The homogeneous circulation of Ni^{2+} or Ni^{3+} in the spongy LNMO microcubes prevents the advanced development of a passive cover on the electrode surface, leading to a low charge transmission resistance ($R_{ct} = 141$) at first cycle and an increase to 180 at 50th cycle.

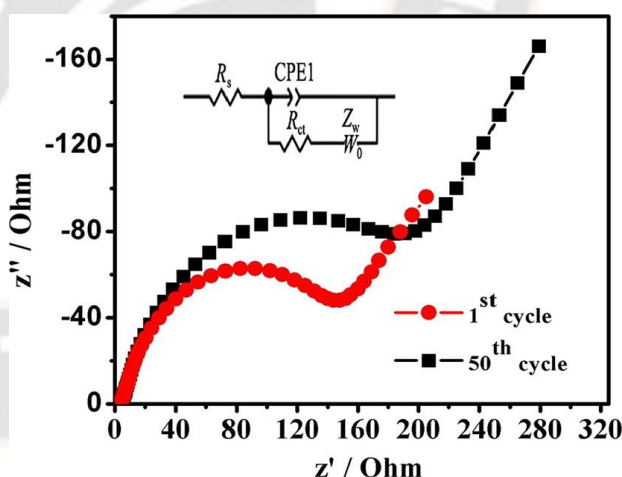


Figure 2.8 Electrochemical impedance spectroscopy of spongy LNMO microcubes

This insulating layer prevents the electrode from dissolving in the electrolyte, making the electrode extremely stable. The electrochemical kinetics response was boosted by the LNMO's porous architecture, which allowed for the diffusion of additional electrolytes on the inner surface. The energy density and discharge plateaus of the cathode materials made of

porous LNMO microcubes were found to be much greater. However, at this point in time, due to the larger charge potentials, the presentations of spongy LNMO nanocubes are still poorer to Li_{0.5}Mn₂O₄. This highlights the need of optimizing the electrolytes in future research into lithium ion batteries.

3. CONCLUSION

The field of "nanotechnology" offers excellent potential for transforming fundamental research into effective technologies. Not just to increase the industry's competitiveness, but also to develop new goods that will improve the lives of our people, whether in the fields of technology, medicine, the environment, or any other.

Nanotechnologies and Nano science open up new research directions and produce innovative, beneficial, and occasionally surprising applications. Products with improved performance can be made using new materials and surfaces with advanced engineering.

According to this study, we have positively synthesized crystal-like and spongy LNMO nanocubes by a simple precipitation process method.

- Carbonate and sulphate acts as structure directing substances that affect the morphology of LiNi_{0.5}Mn_{1.5}O₄, supporting the formation of LNMO microcubes.
- XRD studies confirm the group Fd-3m position of the LNMO sample.
- The FE-SEM and TEM image show that the average size of the porous LNMO microcubes is approximately 163 nm.
- Battery studies show a high discharge capacity (138.4 mA h g⁻¹) in the first cycle and after 50 series by 1.0C, columbic proficiency & volume holding are approximately 93.1% and 74.2% respectively.
- Tremendous electrochemical properties benefit from the porous structure of LNMO, which facilitates the transport of lithium-ion and increases the zone among the electrode & electrolyte.

REFERENCES

1. Singh A V, Laux, P. Luch A, Sudrik, C, Wehr, S, Wild A.-M. et al (2019) Review of emerging concepts in nanotoxicology: opportunities and challenges for safer nanomaterial design. *J. Toxicol. Mech. Methods* 29, 378–387
2. Nikalje AP (2015) Nanotechnology and its Applications in Medicine. *Med chem* 5: 081-089. doi:10.4172/2161-0444.1000247
3. Bertrand N, Leroux JC (2012) The journey of a drug-carrier in the body: an anatomo-physiological perspective. *J Control Release* 161: 152-163.
4. Nagy ZK, Balogh A, Vajna B, Farkas A, Patyi G, et al. (2012) Comparison of electrospun and extruded Soluplus®-based solid dosage forms of improved dissolution. *J Pharm Sci* 101: 322-332.
5. Davide B, Benjamin LD, Nicolas J, Hossein S, Lin-Ping Wu, et al. (2011) Nanotechnologies for Alzheimer's disease: diagnosis, therapy and safety issues. *Nano medicine: Nanotechnology, Biology and Medicine* 7: 521-540.
6. Huston, M.; DeBella, M.; DiBella, M.; Gupta, A. Green Synthesis of Nanomaterials. *Nanomaterials* 2021, 11, 2130.
7. Devatha, C.P.; Thalla, A.K. Chapter 7—Green Synthesis of Nanomaterials. In *Synthesis of Inorganic Nanomaterials*; Mohan Bhagyaraj, S., Oluwafemi, O.S., Kalarikkal, N., Thomas, S., Eds.; Woodhead Publishing: Sawston, UK, 2018; pp. 169–184
8. Wegner, K.; Schimmöller, B.; Thiebaut, B.; Fernandez, C.; Rao, T.N. Pilot Plants for Industrial Nanoparticle Production by Flame Spray Pyrolysis. *KONA Powder Part. J.* 2011, 29, 251–265.
9. Amendola, V.; Meneghetti, M. What controls the composition and the structure of nanomaterials generated by laser ablation in liquid solution? *Phys. Chem. Chem. Phys.* 2013, 15, 3027–3046.
10. Prasad, T.N.V.K.V.; Kambala, V.S.R.; Naidu, R. Phyconanotechnology: Synthesis of silver nanoparticles using brown marine algae *Cystophora moniliformis* and their characterisation. *J. Appl. Phycol.* 2013, 25, 177–182.
11. nadeem baig et al 2021 "Nanomaterials: a review of synthesis methods, properties, recent progress, and challenges", DOI: 10.1039/D0MA00807A (Review Article) *Mater. Adv.*, 2021, 2, 1821-1871